Nov 3rd

Improvements to the Fire Performance of Light Gauge Steel Floor Systems

B. Baleshan

M. Mahendran

Twentieth International Specialty Conference on Cold-Formed Steel Structures
St. Louis, Missouri, U.S.A., November 3 & 4, 2010

IMPROVEMENTS TO THE FIRE PERFORMANCE OF LIGHT GAUGE STEEL FLOOR SYSTEMS

B.Baleshan[1] and M. Mahendran[2]

Abstract

Light gauge steel frame (LSF) structures are increasingly used in commercial and residential buildings because of their non-combustibility, dimensional stability and ease of installation. A common application is in floor-ceiling systems. The LSF floor-ceiling systems must be designed to serve as fire compartment boundaries and provide adequate fire resistance. Fire-rated floor-ceiling assemblies have been increasingly used in buildings. However, limited research has been undertaken in the past and hence a thorough understanding of their fire resistance behaviour is not available. Recently a new composite floor-ceiling system has been developed to provide higher fire rating. But its increased fire rating could not be determined using the currently available design methods. Therefore a research project was conducted to investigate its structural and fire resistance behaviour under standard fire conditions. This paper presents the results of full scale experimental investigations into the structural and fire behaviour of the new LSF floor system protected by the composite ceiling unit. Both the conventional and the new floor systems were tested under structural and fire loads. It demonstrates the improvements provided by the new composite panel system in comparison to conventional floor systems. Numerical studies were also undertaken using the finite element program ABAQUS. Measured temperature profiles of floors were used in the numerical analyses and their results were compared with fire test results. Tests and numerical studies provided a good understanding of the fire behaviour of the LSF floor-ceiling systems and confirmed the superior performance of the new composite system.

Keywords: *Cold-formed steel, LSF Floors, Gypsum plaster board, Fire test, Insulation, Fire rating, Finite element analysis*

[1]PhD researcher, [2]Professor, School of Urban Development, Faculty of Built Environment & Engineering, Queensland University of Technology, Australia.

1.0 Introduction

Cold-formed and thin-walled steel members can be assembled in various combinations to provide cost-efficient and safe light gauge floor systems for buildings. Such Light gauge Steel Framing (LSF) systems are widely accepted in industrial and commercial building construction. Light gauge cold-formed steel joist sections are commonly used in planer structural floor systems with plasterboard on both sides as fire protection. Under fire conditions, thin cold-formed steel sections heat up quickly resulting in rapid reduction to their strength and stiffness. The use of plasterboards provides protection to steel joists during building fires, delaying the temperature rise in the cavity. Fire rating of LSF floor systems is increased simply by adding more plasterboard sheets to the steel joists (the traditional method). Innovative fire protection systems are therefore essential without simply adding on more plasterboard sheets, which is inefficient. According to Sakumoto et al. (2003), the interior (cavity) insulation was found to be increasing the fire resistance of LSF floor panels. However, in the studies of Sultan et al. (1998) and Alfawickhari (2001), floor assemblies without cavity insulation provided higher fire resistance compared to cavity insulated assemblies. Hence the past researches were unable to conclude the effects of traditional approach of using cavity insulation. Recently a new composite LSF wall system was proposed by Kolarkar and Mahendran (2008) at the Queensland University of Technology (QUT) to provide higher fire rating under standard fire conditions**.** They developed a new composite panel system in which insulation was used externally between plasterboards instead of the traditional cavity insulation located within the stud space and investigated its application for LSF wall systems. Such innovations in the plasterboard and insulation systems, steel joist configurations and construction methods have the potential of increasing the fire resistance rating of LSF floor systems. This research therefore proposes that the new composite system is used in ceilings as part of the LSF floor assemblies.

Compared with full-scale fire tests, numerical or finite element analyses (FEA) provide a relatively inexpensive and time efficient alternative. Therefore it can be used to expand the investigation into the behaviour of LSF floor joists under fire conditions without using excessive resources. The numerical analyses of the steel joists were undertaken using the finite element program ABAQUS standard version 6.9 (HKS, 2009) based on the measured temperature profiles obtained from fire tests. Numerical models were calibrated using the full scale test results and were used to further provide a detailed understanding of the structural fire behaviour of LSF floor-ceiling systems. This paper presents the details of the experimental and numerical studies into the thermal and structural performance

of three LSF floor assemblies chosen in this research. Experimental results are presented along with joist failure times and modes and temperatures. Details of the development and validation of a suitable finite element model of LSF floor joists are also presented in this paper.

2.0 Experimental Study

2.1 General

Full-scale fire tests were conducted to investigate the structural and thermal performance of LSF floor systems under fire conditions. Table 1 gives the details of the three full scale floor specimens used in this study. Test specimens were built using four joists, two tracks, two layers of plasterboard and one layer of plywood. The floor area was more than 5 m^2 (2.4m x 2.1m) with a span of 2400 mm, and the floor specimen was simply supported along its two short sides. All the joists and tracks used were fabricated from 1.15 mm G500 galvanized steel sheets. The frames consisted of four joists made of 180 mm deep lipped channel sections as shown in Figure 1. Test frames were made by attaching the joists at the ends to tracks made of unlipped channel sections using 12 mm long self-drilling wafer head screws. Test steel frames were lined on the ceiling side (fire side) by two layers of gypsum plasterboards (16mm) manufactured by Boral Plasterboard under the product name Fire-stop. The face layer of fire side plasterboard was fixed in the same manner as the first layer, but its joints were staggered by 200 mm.

Table1: Details of test specimen configurations

Test	Configuration	Insulation
1		None
2	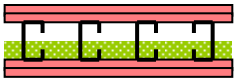	Rock fibre (Cavity insulation)
3		Rock fibre (External insulation)

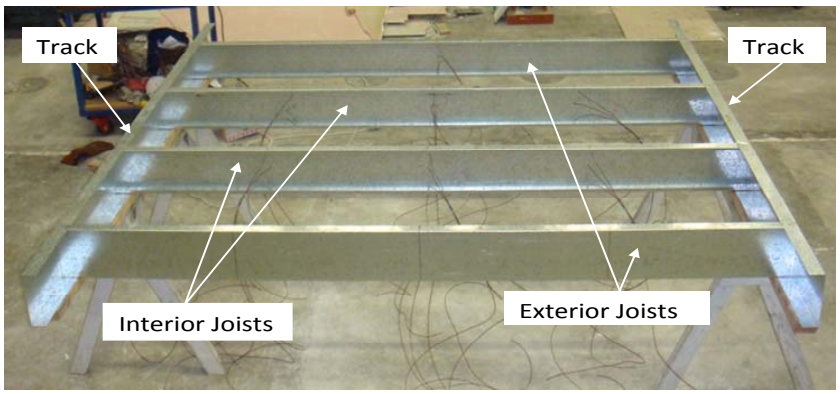

Figure 1: Floor frame

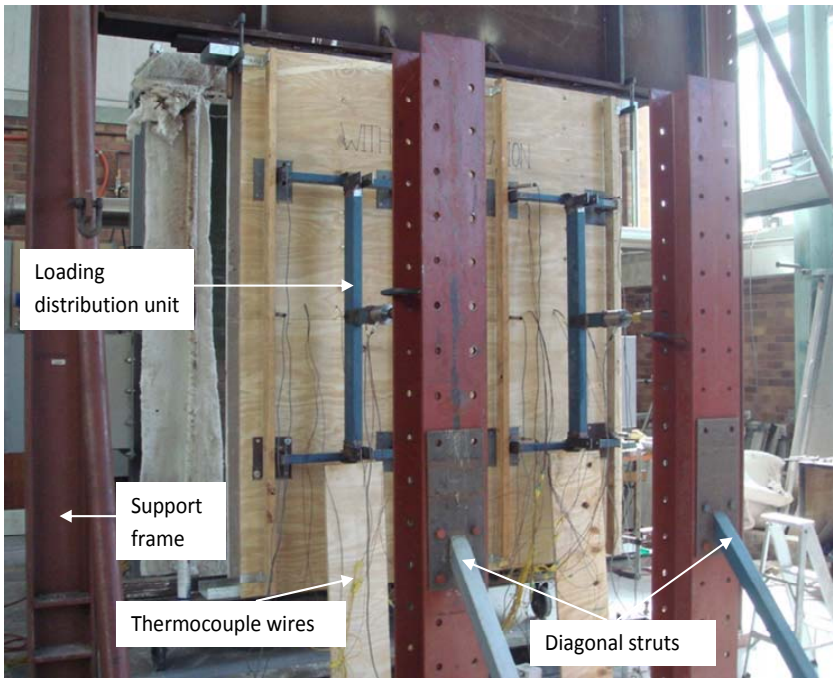

Figure 2: Test set-up

2.2 Test set-up

A heavy steel frame was specially constructed to support the test floor specimens. It consisted of two columns firmly bolted to the strong floor and a universal beam connecting the two columns to form an 'H' shaped portal frame (see Figure 2). The gas furnace only allowed test floor specimens to be set in a vertical position. Hence the transverse loads on the floor specimens were applied in a horizontal direction. In order to simulate a uniformly distributed loading present in LSF floor systems, a load distribution system was developed (see Figure 2) and the target load of 18 kN per jack (4.5 kN per loading point) was applied first and maintained throughout the fire test by the two hydraulic jacks. This target load was determined based on a load ratio of 0.4 where the load ratio is the target load in the fire test to the ultimate failure load of the floor specimen at ambient temperature predicted by FEA. The ultimate failure load at ambient temperature was predicted as 20 kN per joist using the AS/NZS 4600 design rules. A propane fired gas furnace was used in this research to undertake full scale fire tests of the three LSF floor specimens. Many Linear Variable Displacement Transducers were used to measure the lateral deflection of the test specimen. K type thermocouples were used to measure the temperature development across the joists. The average temperature rise as measured by these thermocouples served as the input to the computer controlling the furnace according to the standard cellulosic temperature-time fire curve in AS 1530.4.

2.3 Structural and fire behaviour of test specimens

In all the specimens, at the end of 4 minutes of starting the furnace, smoke was seen coming out from the top of the floor specimen due to the burning of the plasterboard paper on the exposed surface. After about 10 minutes thick smoke and steam were seen to escape from the outer edges from the top of the floor (see Figure 3 (a)). The presence of steam in the mixture of escaping gases was evident as heavy condensation of steam into water was clearly seen on the bottom flange, web of the top UB of the support frame and the top track of the specimens. There were periods of more smoke from the specimens for almost 30 to 40 minutes. This would probably indicate the burning of inside plasterboard paper.

From the beginning of the fire test, the floor specimens were observed to be bending towards the furnace. This continued until the failure and resulted in failing towards the furnace (see Figure 3 (b)). The lateral deflection was the largest in Test Specimen 2 with cavity insulation compared with Test Specimens 1 and 3 (external insulation and no insulation). This was due to higher temperature difference between hot and cold sides of the joists which caused noticeable higher thermal bowing in this test compared with other two tests.

Maintaining the load on the floor specimen was difficult at failure stage with the hand pump controlling the jacks being operated more frequently. The failure was sudden in all the specimens with the joists buckling in the inward direction. The ambient surface of floor specimen recorded temperature values well below the insulation failure temperature (140°C) during all three tests. The failure of the specimen was due to the structural failure of the joists.

(a) Smoke and steam escaping from the top side (b) Lateral deflection of the specimen

Figure 3: Structural and fire behaviour

2.4 Joist temperatures and failure

The failure of the specimens was always by the structural failure of the joists and not by insulation or integrity failure. In the case of cavity insulated specimen, the external plasterboards collapsed prior to joist failure thus hastening the collapse of the floor specimen by exposing the steel frame to direct furnace heat.

Table 2 gives a comparison of the thermal responses of the interior joists at the end of 30, 60, 90 and 120 minutes. Also temperature values are given at the respective failure time of each specimen. Joists of Specimens 1 and 2 reached higher temperatures compared to those in Specimen 3. This is because of the external insulation used in Specimen 3. The cold flange temperature values near the failed interior joists of Specimens 1 and 2 were 320°C and 105°C, respectively. The hot flange failure temperatures of these interior joists are very close to each other (i.e. 489°C). For these joists the temperature differences between hot and cold flanges were 143°C and 398°C, respectively. This may mean that joist failure is mostly governed by the (maximum) hot flange

temperature than the temperature difference between hot and cold flanges. Hence we can conclude that structurally similar LSF floor panels will fail once their joists reach a particular temperature and the fire resistance can be increased only by delaying the maximum temperature in the joists. This is confirmed by the increase in fire resistance time of Specimen 3, which was achieved by the delay in temperature rise in joists due to the use of external insulation.

As seen in Table 2, failure times (fire rating) of Test Specimens 1 to 3 were 107, 99 and 139 minutes. Hence these results demonstrate the improvements to fire resistance of LSF floors by the use of external insulation as proposed in this research. The results also showed that the use of cavity insulation was detrimental to fire resistance of LSF walls in comparison to not using it. In all three cases, failure was due to structural failure of joists by buckling inwards.

Table 2: Thermal responses of interior joists of all three specimens

	Test Specimen 1		Test Specimen 2		Test Specimen 3	
Time (min)	HF (^oC)	CF (^oC)	HF (^oC)	CF (^oC)	HF (^oC)	CF (^oC)
30	121	73	131	63	75	50
60	208	84	236	78	109	75
90	392	226	450	96	152	87
99	-	-	504	106	-	-
107	489	343	-	-	-	-
120	-	-	-	-	298	164
139	-	-	-	-	379	236

3.0 Numerical Study

3.1 General

A numerical study was performed to gain further insight into the buckling and ultimate strength behavioural effects of LSF floor joists under fire conditions, and to investigate the influence of key parameters on their fire resistance. Many finite element analysis programs are currently available. In this research, ABAQUS standard version 6.9 (HKS, 2009) was used for the analysis code. Considerable amount of time was spent in developing an appropriate finite element model for LSF floor joists under fire conditions. In the structural modelling of LSF floor systems, only the individual joists with appropriate loading and boundary conditions were used. The loading simulated the bending

action of joist under the applied transverse loads. In the experimental study, the end conditions were maintained as simply supported. Hence in the numerical study also the support conditions were modelled as simply supported.

3.2 Finite element type and mesh

Element type should be defined correctly to simulate true member behaviour. Based on convergence studies, shell element, S4R, was selected as the most suitable element which can explicitly model the behaviour of LSF joist sections subject to large deformations at higher temperatures. Appropriate selection of mesh size is critical in finite element analysis for improved accuracy of results. A fine mesh density is desirable for greater accuracy, but it may lead to excessive computation time and resources. Also, the aspect ratio of an element (length/width) may have an influence on the solution performance. It was found that a 5 mm x 5 mm (approximately) finite element mesh provides adequate accuracy in modeling the behaviour of joists.

3.3 Symmetry and boundary conditions

The symmetry is considered about a particular axis or a plane of a structure with respect to geometry, boundary conditions and loading patterns before and after the deformations. In the case of support conditions, only one support provides restraint against X-axis translation while keeping other degrees of freedom same. However, it can be considered as symmetrical about the mid-plane. Therefore it was possible to consider only half the span of the test beam, and apply the boundary conditions as shown in Figure 4 to all the nodes at its mid-span. The X-axis translation was prevented at the mid-span cross-section.

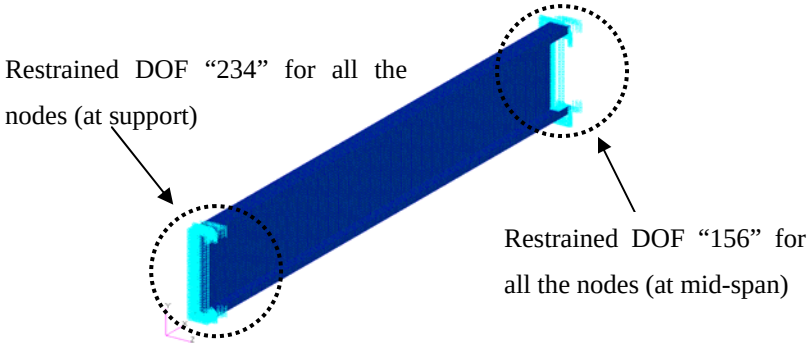

Figure 4: Boundary conditions at the support and mid-span of half-length experimental finite element model

The degrees of freedom notation “123” corresponds to translations in x, y and z axes whereas “456” relate to rotations about x, y and z axes, respectively.

Additional restraining effect provided by plasterboard lining on both sides of the joist was taken into account. For this purpose, the connection of steel joist with plasterboard was represented by a boundary condition restraining the lateral displacement of top and bottom flanges at 300 mm and 200 mm intervals, respectively, which represent the screw fastening locations. This boundary condition was applied to a single row of nodes across the section as shown in Figure 5.

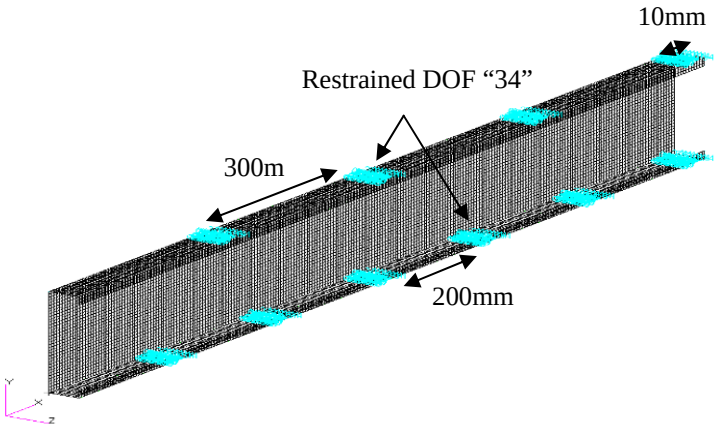

Figure 5: Lateral restraints provided by plasterboard

3.4 Loading conditions

Structural loading

The loading conditions used in the fire tests were simulated in the numerical model. A uniformly distributed loading was simulated as equal concentrated nodal loads over the upper flange of the joist.

Temperature loading

The temperature loading was created as amplitude curve with respect to step time. An amplitude curve allows arbitrary time variations of temperature to be given throughout a step (using step time) or throughout the analysis (using total time). ABAQUS offers different ways to define an amplitude curve: Tabular definition method was selected to define the measured temperature loading amplitude curve as a table of values at convenient points on the time scale. ABAQUAS interpolates linearly between these values, as needed. The temperature loads with time were created using *AMPLITUDE, NAME=name,

DEFINITION=TABULAR option. The temperatures of the steel joist profile at mid-length and quarter points were measured during the fire test. Measured average temperature values (see Figures 7(a)-(c)) were input to the model at three heights over the cross-section (cold flange, web and hot flange) and these temperatures were assumed to be constant over the beam length. The temperature inputs across the section are shown in Figure 6.

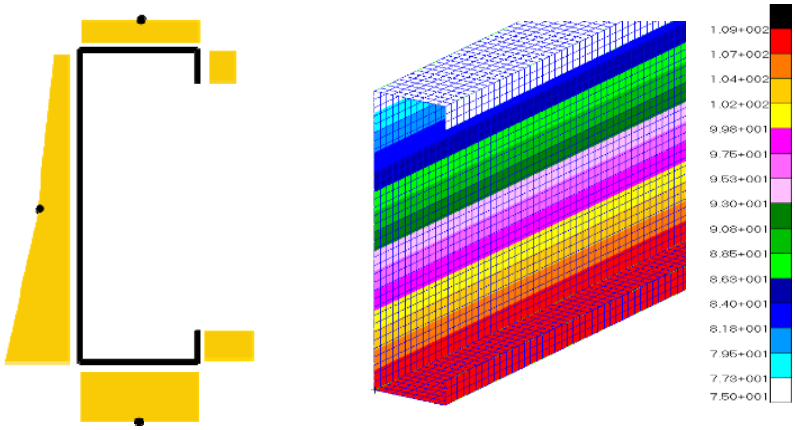

(a) Temperature measurement locations and input

(b) Temperature contours in FEA

Figure 6: Temperature loading across the section

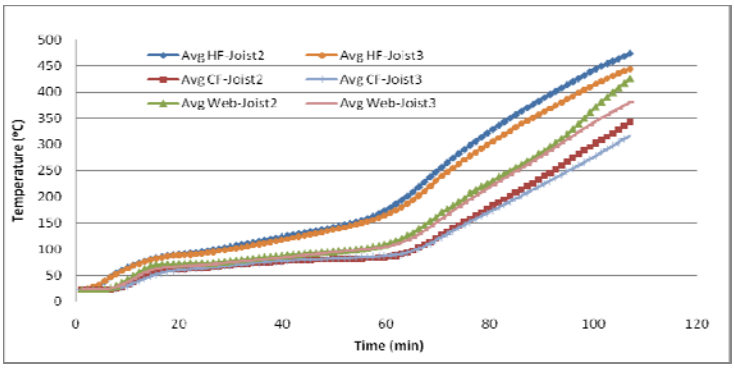

(a) Test Specimen 1

Figure 7: Measured Average Time - Temperature plots of flanges and web surfaces of joists

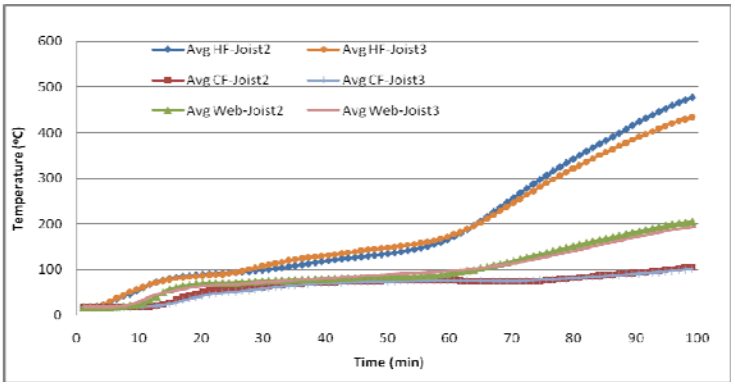

(b) Test Specimen 2

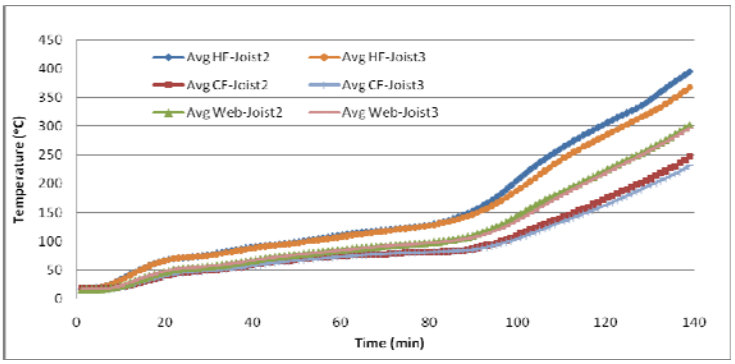

(c) Test Specimen 3

Figure 7: Measured Average Time - Temperature plots of flanges and web surfaces of joists

3.5 Material modeling

The mechanical properties are one of the most important factors in numerical simulations. The mechanical properties required for elastic and nonlinear analyses are Young's modulus of elasticity, yield strength and Poisson's ratio. They should be the same as those of tested specimens to verify the accuracy of developed finite element models. Therefore the yield strength values were

measured using tensile coupon tests at ambient temperature and these measured yield stresses were used in this model. The measured yield strength was 612 MPa while the modulus of elasticity was 210260 MPa, and they were used in the validation of ambient temperature test results. ABAQUS classical metal plasticity model was adopted in this research to include the material non-linearity effects. The reduction of mechanical properties at elevated temperature significantly influences the numerical analysis results. Therefore the mechanical properties should be explicitly considered in the finite element analyses for elevated temperatures. Dolamue Kankanamge (2009) undertook a study to investigate the mechanical properties (yield strength and elastic modulus) of cold-formed steels at elevated temperatures. Her predictive equations were used to determine the yield strength and elastic modulus of 1.15 mm G500 steel at elevated temperatures. The Poisson's ratio was taken as 0.3 and was assumed to remain unchanged with increasing temperature as stated in Ranby (1999). Also the coefficient of thermal expansion was taken as a constant value of 0.000014 $°C^{-1}$ even at higher temperatures.

The initial geometric imperfection values used in the previous studies varied among the past studies. Both local and global initial geometric imperfections were included in Schafer and Pekoz (1997). On the other hand an imperfection amplitude value of L/1000 was used in the studies of Kaitila (2002). However, due to the dominance of thermal bowing the effect of initial geometric imperfection does not have any significant effect on the behaviour of LSF joist at elevated temperature. The geometric imperfections in the joists were applied by modifying the nodal coordinates using a field created by scaling appropriate buckling eigenvectors obtained from an elastic bifurcation buckling analysis. The lowest buckling eigenmodes are usually the critical mode. Hence, a value of b/150 was used in this model after considering the modes from the bifurcation buckling analysis of LSF joists at ambient condition. Residual stresses diminish rapidly with increasing temperature. Therefore the effect of residual stresses was considered to be negligible at elevated temperatures in this model.

3.6 Validation of experimental finite element models at ambient conditions

In the ambient condition, joists were considered as fully laterally restrained by plasterboard and plywood at the top and bottom flanges. Therefore flexural capacity calculations from AS/NZS 4600 were used to validate the results of FEA at ambient condition. This is to ensure that the finite element model can be extended to simulate the desired buckling and ultimate strength behaviour of cold-formed steel joist at fire conditions. The design section moment capacities agree reasonably well with the FEA results as seen in Table 3.

The RIKS method uses the load magnitude as an additional unknown. It solves simultaneously for loads and displacements. Therefore another quantity must be used to measure the progress of the solution. ABAQUS uses the "arc length," along the static equilibrium path in load-displacement space (HKS, 2009). This approach provides solutions regardless of whether the response is stable or unstable. Large displacement theory was also considered in the analyses.

Table 3: Moment capacities of joists from FEA and design codes

Ultimate moment capacity (FEA-Non linear)	6.89 kNm
Section moment capacity (AS 4600)	5.98 kNm
Section moment capacity (Euro code)	6.68 kNm

3.7 Validation of experimental finite element models under fire conditions

Deflection curves

The finite element modelling was performed under dynamic condition where the joist was first subjected to the pre-determined applied load and then it was exposed to the measured temperature profiles. Finite element analyses were performed in three static analysis steps. The first step was an eigen buckling analysis at ambient condition, in which the buckling modes were obtained and the deformed profile of the lowest buckling mode was used to determine the joist initial imperfection. Nonlinear analyses were then performed for the remaining steps with Riks-off method. In the second step, the load was applied incrementally up to the target level. Temperature was then applied in the final step to follow the measured temperature profiles. The accuracy of the developed finite element models was validated using the time-lateral deflection curves obtained from the full scale fire tests. Figures 8 (a)-(c) show a close agreement between the deflection curves from fire tests and FEA. The agreement of these curves is very good compared to the previous numerical studies of LSF floors under fire conditions.

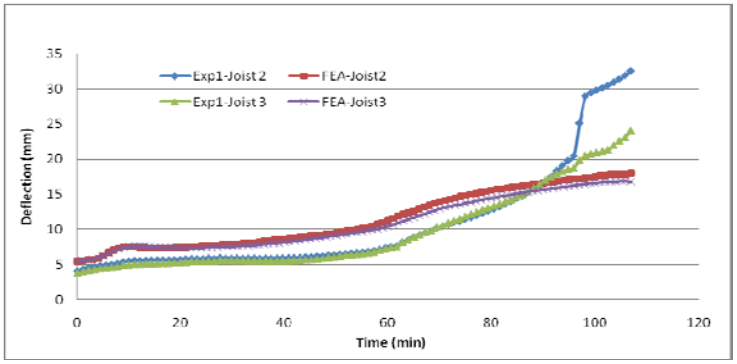

(a) Test Specimen 1

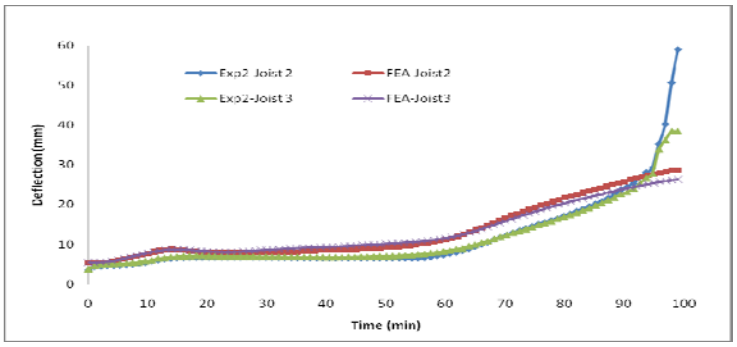

(b) Test Specimen 2

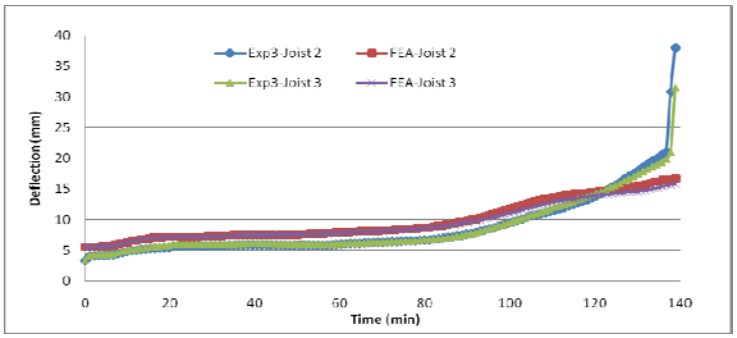

(c) Test Specimen 3

Figure 8: Lateral deflection plots obtained from fire tests and FEA

Failure modes

It was noted that flexural-torsional buckling and flexural buckling about the minor axis of joist were fully prevented by the lateral support offered by the dual layers of plasterboard throughout the test. The central joists in all the specimens experienced local failures at the support as shown in Figure 9 (c). Figure 9 (a) shows the failure mode of the joist where the local buckling waves were observed along the length. Figures 9 (a)-(c) show close agreement of the failure modes between experiment and FEA near the ultimate failure point.

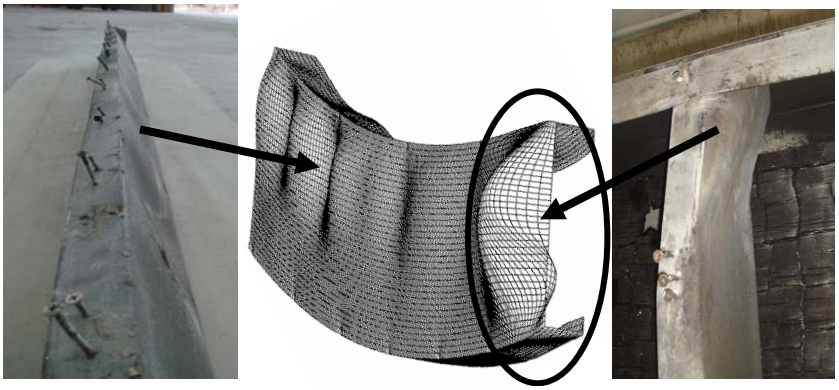

(a) Local web buckling along joists (b) Failure modes in FEA (c) Local failure at support

Figure 9: Failure modes of joists from Fire Tests and FEA

Predictions of failure times

For the convenience of comparison of FEA failure time with experimental failure time, the finite element analyses were performed under the steady-state condition in two steps. This means the temperature distributions in the steel cross-section are raised to the target levels and then kept unchanged in the first step. Following this, the load was applied in increments until failure with Riks-on in the next step. The joist temperatures are based on the measurements of joist temperatures at different times during the fire tests. Figure 10 shows the predicted failure times from FEA. From Figure 10, failure times can be predicted for the three fire tests based on the applied moment of 2.81 kNm and the results are given in Table 4. Table 4 results confirm that the failure times predicted by FEA agree reasonably well with the results from the fire tests.

Table 4: Failure times from experiments and finite element analyses

Test	Insulation	Failure Mode	Failure Time Expt. (min)	Failure Time FEA (min)
1	None	Structural	107	110
2	Rock fibre Cavity insulation	Structural	99	106
3	Rock fibre External insulation	Structural	139	156

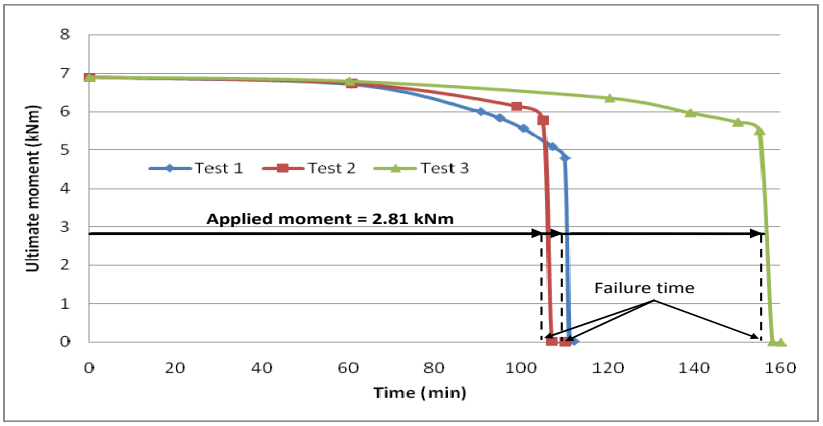

Figure 10: Failure time prediction

4.0 Conclusions

This paper has presented the details of three full scale fire tests of a new light gauge steel floor-ceiling system using external insulation and the results. This study has shown that the use of cavity insulation led to poor thermal and structural performance of LSF floors. In contrast, the thermal and structural performance of externally insulated LSF floor system was superior than the traditionally built floors with or without cavity insulation. Details of fire tests and the results are presented and discussed in this paper. The numerical models were developed and validated to fully understand the improvements offered by the new composite system and to confirm the fire test observations. The use of accurate numerical models allowed the inclusion of various complex thermal

and structural effects such as thermal bowing, local buckling and material deterioration at elevated temperatures.

Acknowledgment

The authors would like to thank Australian Research Council for the financial support to this project and the Queensland University of Technology for providing the necessary facilities and technical support.

References

Alfawakhiri, F. (2001), Behaviour of Cold-Formed-Steel-Framed Walls and Floors in Standard Fire Resistance Tests, PhD Thesis, Faculty of engineering, Carleton University, Ottawa, Ontario, Canada.

Baleshan, B. Mahendran, M. (2010), Full Scale Fire Tests of a New Light Gauge Steel Floor-Ceiling System, Proc. of the 4th International Conference on Steel and Composite Structures, Sydney, Australia. (Paper submitted)

Dolamue Kankanamge, N. (2009), Structural Behaviour and Design of Cold-formed Steel Beams at Elevated Temperatures, PhD Thesis, Queensland University of Technology, Brisbane, Australia.

European Committee for Standardization (CEN) Eurocode 3 (1996) ENV 1993-1-3, Design of Steel Structures, General Rules- Supplementary Rules for Cold-formed Thin Gauge Members and Sheeting, London, UK.

Hancock, G.J. (2005), Design of cold-formed steel structures, Australian Institute of Steel Construction, Sydney, Australia.

Hibbitt, Karlsson & Sorensen, Inc. (HKS) (2009). ABAQUS User's Manual, Hibbitt, Karlsson & Sorensen, Inc., Rhode Island, USA.

Kaitila, O. (2002), Finite Element Modelling of Cold-Formed Steel Members at High Temperatures, Licentiate of Science in Technology Thesis, Helsinki University of Technology, Finland.

Kolarkar, P. and Mahendran, M. (2008), Thermal Performance of Plasterboard Lined Stud Walls, Proc. of 19th International Specialty Conference on Cold-Formed Steel Structures, St. Louis, Missouri, U.S.A, pp.517-530.

MSC. Patran (2008). Patran Version 2008 r1, MSC.Software Corporation, California, USA.

Ranby, A. (1999), Structural Fire Design of Thin Walled Steel Sections, Licentiate Thesis, Division of Steel Structures, Department of Civil and Mining Engineering, Lulea University of Technology, Sweden.

Sakumoto, Y., Hirakawa, T., Masuda, H. and Nakamura, K. (2003), Fire Resistance of Walls and Floors Using Light-Gauge Steel Shapes, Journal of Structural Engineering, pp.1522-1530.

Schafer, B.W. (1997). Cold-formed Steel Behavior and Design: Analytical and Numerical Modeling of Elements and Members with Longitudinal Stiffeners, Ph.D. Thesis, Cornell University, Ithaca, New York, USA.

Standards Australia (SA) (2005), AS/NZS 4600, Cold-formed Steel Structures, Sydney, Australia.

Standards Australia (SA) (1997), AS 1530.4, Methods for fire tests on building materials, components and structures, Sydney, Australia.

Standards Australia (SA) (1998), AS/NZS 2588, Gypsum Plasterboard, NSW, Australia.

Sultan, M.A., Seguin, Y.P., Leroux, P., MacLaurin, J.W and Monette, R.C. (1998), Temperature Measurements in Full-Scale Fire Resistance Tests on Insulated and non-insulated Steel Joist Floor Assemblies, Internal Report, Institute for Research in Construction, National Research Council of Canada, Ottawa, Ontario, Canada.

VTT (2001), Fire resistance test on a load-bearing, separating floor construction, Test Report No.RTE3819/00, Technical Research Centre of Finland (VTT), Espoo, Finland.